Liquid Phase Oxidation Kinetics of Oil Sands Bitumen: Models for *In Situ* Combustion Numerical Simulators

Multiresponse kinetic models are established for the low-temperature oxidation (LTO) reactions of Athabasca oil sands bitumen. The models provide adequate description of the overall rate of oxygen consumption and of the reactions of the liquid phase bitumen components. The LTO models are suitable for use in the *in situ* combustion numerical simulators of the oil sands.

K. O. Adegbesan
Texaco Canada Resources Ltd.

J. K. Donnelly
BP Exploration Canada Ltd.

R. G. Moore, D. W. Bennion
Department of Chemical and
Petroleum Engineering
The University of Calgary
Calgary, Alberta T2N 1N4, Canada

SCOPE

Several articles have been published describing *in situ* combustion techniques and giving detailed results of laboratory and field experiments. These papers include: Alexander et al. (1962), Bennion et al. (1977), Burger and Sahuquet (1973), Cram and Redford (1977), Dietz (1970), Dietz and Weidjema (1968), Morse (1976), Nelson and McNiels (1956), Showalter (1963), Smith and Perkins (1973), Reed et al. (1960), and Walter (1977). The performance of *in situ* combustion processes depends on the accompanying low-temperature oxidation (LTO) reactions (Alexander et al., 1962; Dabbous and Fulton, 1974; Burger and Sahuquet, 1973). Furthermore, results of published laboratory and field studies indicate that more meaningful analysis of combustion data cannot be made until the LTO reaction kinetics are studied and the reaction mechanisms elucidated. Consequently, a reliable numerical simulator of the *in situ* combustion processes must model adequately the LTO reactions. The simulator should include an LTO reaction model able to do the following:

1. Represent the overall rates of oxygen consumption
2. Represent the major reaction components and products in the liquid phase and their individual rates of transformations.

Reported studies of LTO reactions of oil sands bitumen have been qualitative in nature (Moschopedis and Speight, 1975, 1976a, b, 1977). Other published studies have considered only the overall rates of oxygen consumption for LTO reactions of conventional crude oils (Dabbous and Fulton, 1974; Fassihi et al., 1980; Morton and Bell, 1958).

The main objective of this study is the construction of adequate multiresponse kinetic models for use in numerical simulators of *in situ* combustion. For this purpose, a semiflow reactor was designed and used to gather intrinsic and isothermal kinetic data. Details of the reactor, the experimental system and kinetic data have been presented elsewhere (Adegbesan, 1982).

To simplify and make practical the representation of the LTO reactions, characterization of the reaction network was achieved using a component lumping tech-

---

Correspondence concerning this paper should be addressed to K. O. Adegbesan, who is now with Esso Resources Canada Ltd.

nique (Adegbesan, 1982). Efforts were directed toward building mechanistic models rather than empirical ones. Multiresponse kinetic models were developed and the maximum likelihood parameters in the models were estimated. Due to coupling of chemical reaction and solubility, an accurate measurement of the solubility of oxygen in oil sands bitumen was not possible. Consequently, the models' kinetic and solubility parameters are coupled. However, our solution techniques provide an estimate of the solubility of oxygen in bitumen and can be applied to decouple the rate parameters. All proposed models were statistically tested for adequacy.

CONCLUSIONS AND SIGNIFICANCE

Multiresponse kinetics models are established for the LTO reactions of oil sands bitumen. Based on experimental kinetic data, two main types of reactions models are proposed. These are:

1. A nonsteady state kinetic model to represent the overall rate of oxygen consumption; this model is second-order with respect to oxygen partial pressure.
2. Four nonsteady state multiresponse kinetic models representing the LTO reactions of the bitumen liquid components. These components include the saturates, the aromatics, the maltenes, the resins, the asphaltenes, and coke. The models are first-order with respect to the lumped components and fractional order in oxygen partial pressure.

Invariant kinetic parameters in the models were estimated using the maximum likelihood techniques. Proposed models were found statistically adequate and are suitable for use in numerical simulators of *in situ* combustion.

Experimental

Apparatus

A diagram of the experimental apparatus is shown in Figure 1. The gas feed system consists of nitrogen and oxygen-nitrogen gas cylinders. Gas feed rates are controlled by variable-area choke nozzles. Product gas from the reactor was passed through a water condenser, an oil condenser, and a fiber filter. Pressure in the reactor was controlled by an automatic backpressure controller and the flow rate of the exit gas was measured by a wet-

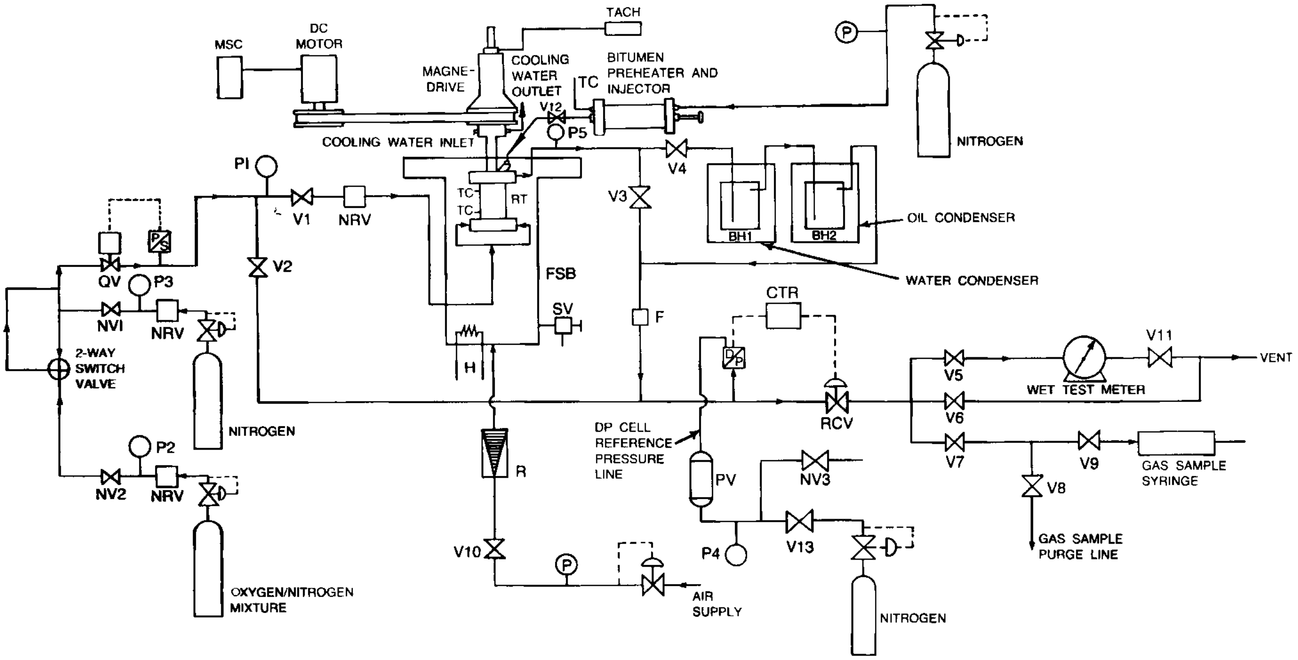

BH1 = Ice-water bath
BH2 = Dry ice-methanol bath
CRT = Pressure controller
CV = Check valve
D/P = Differential pressure cell
F = Fiber filter
FSB = Fluidized sand bed
H = Fluidized-bed heater with controller
MSC = Motor speed control
NV = Needle valve
NRV = No-return valve
P = Pressure gauge
P/S = Pressure switch
QV = Quick mechanism valve
R = Rotameter
RT = Reactor
RCV = Research control valve
SV = Fluidized-bed sand valve
TACH = Tachometer
TC = Thermocouple
V = Regulating valve

Figure 1. The flow system.

test meter. Gas samples of the reactor exit gas were taken periodically and analyzed by gas chromatography.

A magnetically coupled stirred reactor was used for this study. The reactor was of type 316 stainless steel and had a 34.9×10^{-3} m ID and a length of 190.0×10^{-3} m. An Autoclave Engineer's MagneDrive II unit driven by a variable speed DC motor allowed for high-pressure stirring without gas leakage problems. Two chromel-alumel thermocouples were used to measure the temperatures in the reactor. The reactor was eqipped with bitumen injection ports and valves. A nitrogen-driven floating-piston injector was used to inject bitumen into the reactor at the start of each run. Feed gas was injected into the liquid phase using a sintered stainless steel plate having an average pore size of 20 microns. Dispersion of gas into the liquid phase was achieved by rotating a six-bladed standard turbine impeller. A six-bladed baffle was used in each reactor to improve the contact efficiency.

The reactor was heated using a fluid bed and was cooled by a cold water bath, mounted on a swivel platform. The platform level was controlled by two hydraulic pistons.

Preparation of bitumen sample

The preparation technique of the bitumen sample used in this study is described in a paper by Vorndran et al. (1980). The sample of oil sand was obtained from Suncor in Fort McMurray. The oil sand was taken from the mine face at the bottom of the second face. It was divided and put into plastic bags that were then sealed in metal containers and kept frozen. Samples were randomly selected and extracted using modified Soxhlet extractors with toluene as the solvent. All bitumen used in this study was obtained in a single extraction operation.

Kinetic study

The experimental procedure consisted of preheating the reactor to the desired test temperature, establishing the desired gas flow rate and stirrer speed, and injecting a bitumen sample into the reactor. The reactor was maintained at the desired temperature for a predetermined time and then quenched in the cold water bath. The oxidized oil was removed and analyzed for density, viscosity, and composition (SARA analysis). Tests were conducted at set temperatures and at varying time intervals for each temperature. The oxygen content of the feed gas was also varied over the range 0.98–50.87%. A detailed discussion of the experimental procedure is presented elsewhere (Adegbesan, 1982).

Fractionation of the original and the oxidized bitumen

In this study, the SARA analysis scheme was used to separate the original and the oxidized bitumen into pseudocomponents. Two major sets of apparatus used in this study are a modified Soxhlet extractor and a silica gel/alumina column.

The modified Soxhlet extractor is similar to that used by Vorndran et al. for core analysis. The silica gel/alumina column is similar to that described by Bulmer and Starr (1979). The experimental procedure used is similar to that published by Moschopedis and Speight (1976a) for fractionation of bitumen and has been modified and extended to fractionate oxidized bitumen in this study. The separation scheme is shown in Figure 2; details of separation are presented elsewhere (Adegbesan, 1982). Table 1 summarizes the properties and composition of the original bitumen sample.

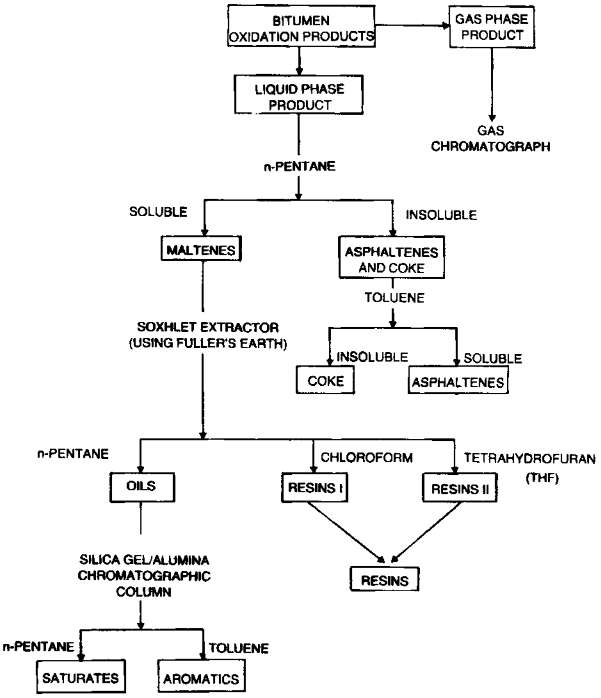

Figure 2. Separation scheme for original bitumen and oxidation products.

Experimental Results

Preliminary tests were carried out at 423 K and an oxygen partial pressure of 885 kPa (total pressure of 4,415 kPa) in order to determine the gas flux and stirring rates required to ensure operation in the kinetic subregime. Tests were also conducted to determine the effect of the reactor material and extracted oil sands on the kinetics data. The following were concluded:

- Type 316 stainless steel and bitumen sands (mostly fines) had no catalytic influence on the rates of reaction of lumped components of bitumen.

Table 1. Properties and Composition of Natural Athabasca Bitumen

Specific Gravity	
298 K	1.0138
Viscosity	mPa · s
368 K	455
383 K	205
Elemental Analysis	mass %
Carbon	83.47
Hydrogen	10.21
Sulfur	4.44
Oxygen	2.25
Nitrogen	0.49
SARA Components	mass %
Resins I	18.95
Resins II	8.81
Oils	47.83
Asphaltenes	20.36
Coke	0.00

- All mass transfer limitations were eliminated at gas fluxes over $6.667 \times 10^{-2} m^3 \cdot m^{-2} \cdot s^{-1}$ STP and at impeller speeds over 2,400 rpm.

Once the operating conditions were established, a series of isothermal runs were carried out at 423, 408, 393, 378, and 333 K. The inlet oxygen partial pressure ranged from 40 to 2,233 kPa.

Concentration vs. reaction time curves of kinetic reactions at 408 K are presented in Figure 3. These data indicate that the LTO reactions of bitumen consist of a series of consecutive steps resulting in the formation of the asphaltenes-coke component from the oils, with the resins as the intermediate components. Similar behavior was observed for the kinetic reactions carried out at the other temperatures.

Significant observations arising from the experimental work are the following:

1. Marked changes occurred in the properties of natural bitumen when subjected to oxidation. Both the density and apparent viscosity increased with severity of oxidation. Oxidized bitumen viscosities were orders of magnitude higher than those of the original material. Figures 4 and 5 show the effect of oxidation on the viscosity and density of original bitumen, respectively.
2. The oxidation of maltenes resulted in the formation of the asphaltenes-coke components. Oxidation of the asphaltenes resulted in a high yield of toluene insoluble material (coke).
3. No significant effect of total pressure on reaction rates was observed.
4. Oxygen partial pressure had a relatively strong influence on the overall rate of oxygen consumption and a lesser effect on the oxidized oil composition. Figure 6 summarizes the effect of oxygen partial pressure at 423 K. Similar behavior was observed at other temperatures.

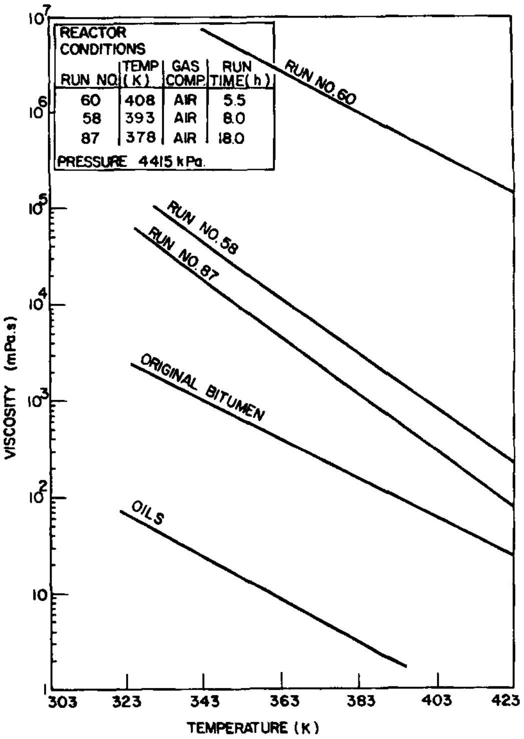

Figure 4. Effect of LTO on viscosity of Athabasca bitumen.

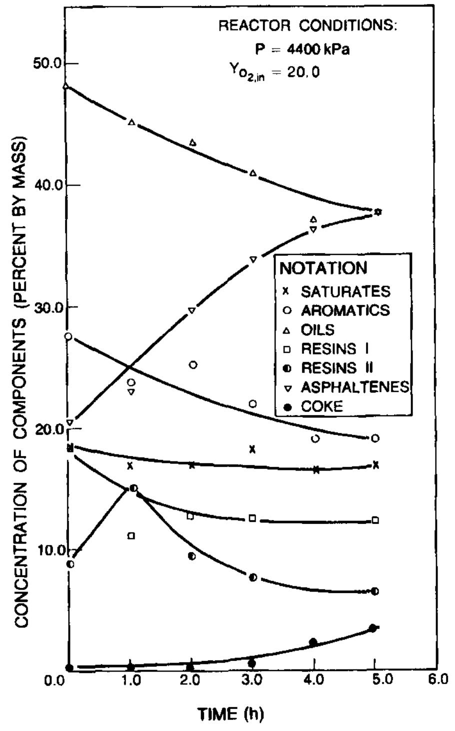

Figure 3. Conversion of bitumen at 408 K.

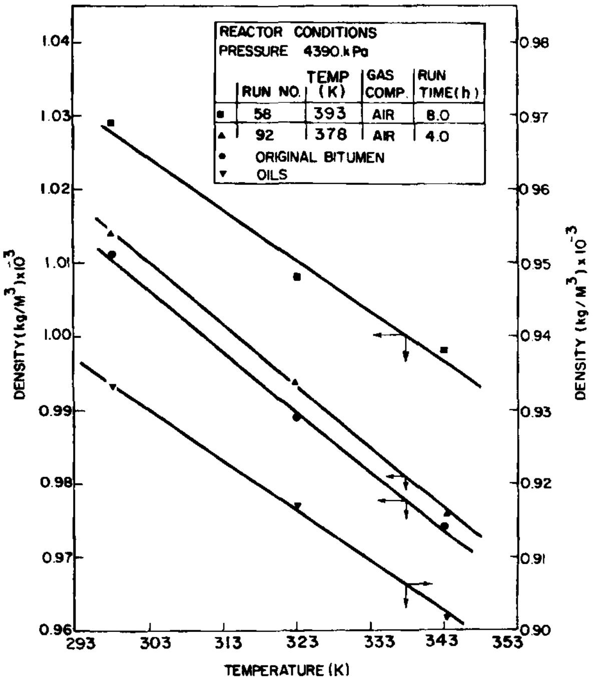

Figure 5. Effect of LTO on density of Athabasca bitumen.

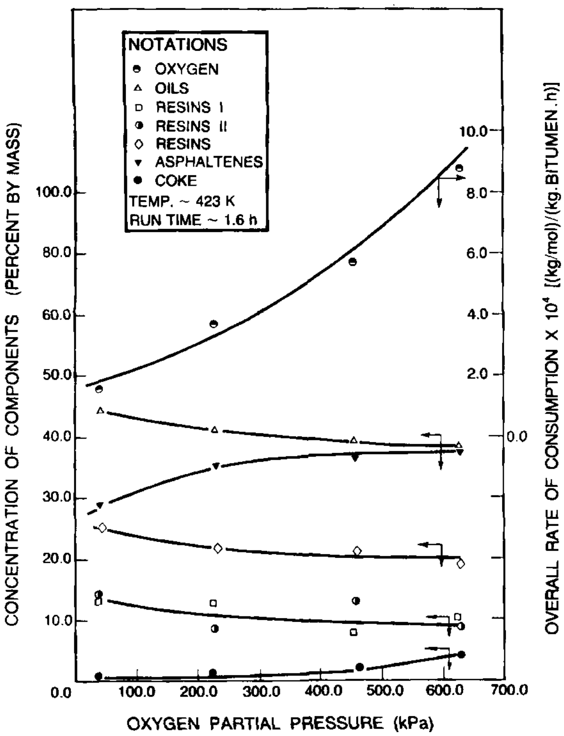

Figure 6. Effect of oxygen partial pressure on reaction rates.

5. Analysis of the reactor exit gas showed that carbon oxides were the only reaction products in the gas phase. Carbon oxides were present only in the 418 and 423 K tests.

6. Overall rates of oxygen uptake increased rapidly during the early stages of the reaction, reached a peak, and then declined gradually. Steady state compositions were not attained over the reaction periods considered.

Design Equations for the Semiflow Reactor

A two-phase reactor is classified as a semiflow reactor if the liquid is held within and only the gas flows through the reactor. The reactor configuration used in this study is that of well-mixed gas/well-mixed batch liquid. Both phases are intimately mixed by mechanical agitation and by the action of the gas on the liquid. The concentrations in both phases are assumed to be time-dependent but spatially invariant. Figure 7 illustrates the reactor configuration for this case. The following are the non-steady state general component material balances; details of the derivations of the equations and underlying assumptions are presented elsewhere (Adegbesan, 1982).

Gas phase

Assuming no chemical reactions within the gas phase, an unsteady state general component material balance can be written as:

$$G_1 Y_{oj} - G_2 Y_j - K_G P(Y_j - C_j^* He/P) = \frac{d}{dt}\left(\frac{PV_G Y_j}{zRT}\right) \quad (1)$$

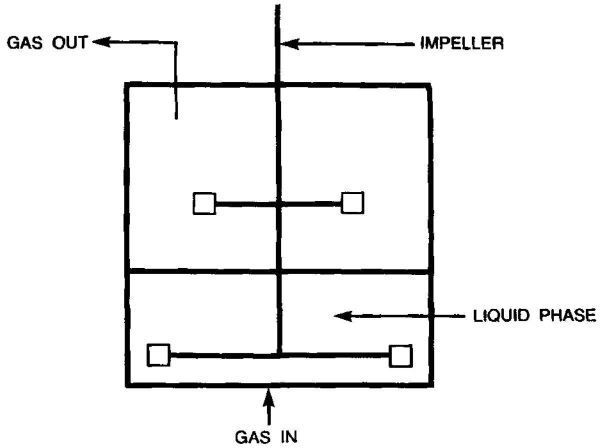

Figure 7. A semiflow reactor configuration.

Liquid phase

$$k_L(C_j - C_j^*) - r_j V_L = \frac{d}{dt}(V_L C_j) \quad (2)$$

Interphase material balance for oxygen

$$G_1 Y_{O_{2,in}} - G_2 Y_{O_{2,out}} + k_L(C_{O_2} - C_{O_2}^*) - r_{O_2} V_L = \frac{d}{dt}[V_L C_{O_2}] \quad (3)$$

Reaction Kinetic Models

Formulation of rate equations

A complete description of the actual mechanism involved in the oxidation reaction of heavy oil or bitumen is usually not attainable and would certainly be hopelessly complex and unsuitable for use in numerical *in situ* combustion simulators. Consequently, characterization of the reaction scheme was achieved only in terms of a limited number of major components using the SARA lumping scheme.

Knowledge of the liquid phase concentration of oxygen is needed to model LTO reactions since reactions occur in the liquid phase. An accurate evaluation of the solubility of oxygen in bitumen will be difficult to measure due to coupling of chemical reaction and solubility. LTO reactions of hydrocarbons are, in general, observed to be relatively slow. Consequently, equilibrium concentration of oxygen can be assumed within the liquid phase. The liquid phase can be considered dilute with respect to its oxygen content; therefore, its oxygen concentration may be represented by Henry's law.

The dependence of the Henry's law coefficient on temperature and pressure is given by Denbigh (1971) as follows:

$$\left.\frac{\partial(\ln He)}{\partial T}\right|_P = \frac{L}{RT^2} \quad (4)$$

$$\left.\frac{\partial(\ln He)}{\partial P}\right|_T = \frac{V}{RT} \quad (5)$$

Where

$$L = -(h^g - H) \quad (6)$$

Equation 4 can be integrated to give:

$$He = Ho \exp(-L/RT) \tag{7}$$

This form of Henry's law is most suitable for use in developing the rate equations.

Proposed Models

Two types of models were proposed, one to account for the overall rate of oxygen consumption (model C-1) and the other to represent the rates of reactions of the bitumen components. Four reaction networks were developed to describe the LTO reactions of bitumen based on two (C-2), three (C-3), and four (C-4A and C-4B) pseudocomponents. These reaction networks were based on experimental data, particularly the time-dependent lumped component distribution curves and the elemental analysis (Adegbesan, 1982).

A summary of the proposed reaction schemes is presented in Table 2. In the following sections, a summary of derivations of the rate expressions is presented for the proposed kinetic models; details of the derivations are documented elsewhere (Adegbesan, 1982).

Overall rate of oxygen consumption (model C-1)

An unsteady state model representing the overall rate of oxygen consumption can be derived from the interphase material balance for oxygen (Eq. 3) by applying the exponential form of Henry's law to represent the liquid phase oxygen concentration. The final form of the rate expression for model C-1 is presented in Table 3. The assumptions made in the formulation of equations for model C-1 include the following:

1. Reactions occurred in the kinetic subregime
2. The total concentration of hydrocarbons, C_H, remained essentially unchanged by chemical reaction
3. The change in density of the liquid phase due to chemical reactions was insigificant.

Table 2. Proposed LTO Reaction Schemes

MODELS	REACTION KINETIC SCHEMES
Overall Rate C-1	Bitumen + Oxygen $\xrightarrow{k'o,\ E'}$ products (overall rate of oxygen consumption)
Reactions of Bitumen Components C-2	$A_1 \xrightarrow{k_{15},\ E_{15}} A_5$ (Maltenes) (Asphaltenes-coke)
C-3	$A_2 \xrightarrow{k_{26},\ E_{26}} A_6 \xrightarrow{k_{65},\ E_{65}} A_5$ (oils) (Resins) (Asphaltenes-coke)
C-4A	$A_2 \xrightarrow{kc_{23},\ Ec_{23}} A_3 \xrightarrow{kc_{35},\ Ec_{35}} A_5$ (oils) (Resins I) (Asphaltenes-coke) $A_2 \xrightarrow{kc_{24},\ Ec_{24}} A_4 \xrightarrow{kc_{45},\ Ec_{45}} A_5$ (oils) (Resins II) (Asphaltenes-coke)
C-4B	$A_2 \xrightarrow{k_{23},\ E_{23}} A_3 \xrightarrow{k_{34},\ E_{34}} A_4 \xrightarrow{k_{45},\ E_{45}} A_5$ (oils) (Resins I) (Resins II) (Asphaltenes -coke)

Table 3. Rate Data for Model C-1

REACTION MODEL	$\frac{dY}{dt} \quad \frac{HoG}{V_L P}(Y_{O_{2,in}} - Y) \exp(-L/RT)$ $-k'o\, Y^{m1} \exp(-E'/RT)$ $k'o \quad koHo^{1-m1},\ E' \quad E + (1 + m1)L$	
	Arrhenius' Law Constants	Henry's Law Constants
Frequency Factors	ko [cm³.mol⁻¹.h⁻¹] 8.066 E + 29	Ho [kPa.cm³.mol⁻¹] 3.678 E + 02
Activation Energy (J/mol)	E 238.422	L 6.774
Rate Constants	k [cm³.mol⁻¹.h⁻¹]	He [kPa.cm³.mol⁻¹]
423 K	4.34 E + 00	1.036 E + 02
408 K	1.279 E + 00	6.853 E + 01
393 K	1.439 E - 02	9.816 E + 00
378 K	9.281 E - 04	3.748 E + 00
333 K	1.850 E - 10	1.835 E - 02
Order of Reaction with Respect to Oxygen Partial Pressure. (mi)	m1 2.0	

Liquid phase lumped-components models (models C-2 to C-4)

As shown in Table 2, the saturates and aromatics components were not represented individually in the reaction schemes. They were lumped together and represented by the oils components. Similarly, the asphaltenes and the coke components were lumped together. The rate expressions for four-component model C-4A can be developed from the unsteady state material balance of Eq. 2. For reaction in the kinetic subregime, and for a constant volume of the liquid phase, a suitable form of the kinetic rate expressions can be obtained by expressing the concentrations of the components in terms of their mass fractions in solutions. They are the following:

$$\frac{dX_{A_2}}{dt} = -[kc'o_{23}X_{A_2}\exp(-Ec'_{23}/RT) + kc'o_{24}X_{A_2}\exp(-Ec'_{24}/RT)]p_{ox}^{m2} \tag{8}$$

$$\frac{dX_{A_3}}{dt} = kc'o_{23}X_{A_2}p_{ox}^{m2}\exp(-Ec'_{23}/RT) - kc'o_{35}X_{A_3}p_{ox}^{m3}\exp(-Ec'_{35}/RT) \tag{9}$$

$$\frac{dX_{A_4}}{dt} = kc'o_{24}X_{A_2}p_{ox}^{m2}\exp(-Ec'_{24}/RT) - kc'o_{45}X_{A_4}p_{ox}^{m4}\exp(-Ec'_{45}/RT) \quad (10)$$

$$\frac{dX_{A_5}}{dt} = kc'o_{35}X_{A_3}p_{ox}^{m3}\exp(-Ec'_{35}/RT) + kc'o_{45}X_{A_4}p_{ox}^{m4}\exp(-Ec'_{45}/RT) \quad (11)$$

Where

$$kc_{\ell j} = kco_{\ell j}\exp(-Ec_{\ell j}/RT) \quad (12)$$

$$kc'o_{\ell j} = Ho^{-mi}kco_{\ell j} \quad (13)$$

and

$$Ec'_{\ell j} = Ec_{\ell j} - miL \quad (14)$$

It must be noted that Henry's law parameters *Ho*, *L* are lumped together with the Arrhenius preexponential factor *kco* and the activation energies *Ec* according to Eqs. 8–11. The actual values of the Arrhenius preexponential factors and the activation energies cannot be estimated unless independent values of the Henry's law parameters are obtained. However, the rate equations of the type developed above are quite convenient for use in *in situ* combustion numerical simulators.

Four-component model C-4B assumes that the resins II are formed directly from resins I and the asphaltenes-coke components are formed directly from resins II. Less complex kinetic schemes can be derived from the four-component models by further lumping the pseudocomponents. In the three-component model, C-3, the resins I and resins II components are combined together to form a single component called the resins. Also, in the two-component model, C-2, the oils and the resins component are further lumped together to form a component called the maltenes. The maltenes concentration data are obtained independently according to the SARA separation scheme.

The rate expressions for models C-4B, C-3, and C-2 were also developed using procedures similar to that applied to model C-4A. The final forms of the rate expressions for models C-2, C-3, C-4A and C-4B are presented in Tables 4 to 7.

Estimation of Parameters

The invariant kinetic parameters in the reaction models were estimated using maximum likelihood parameter estimation techniques (Box and Draper, 1966; Box et al., 1973). Details of the estimation techniques used in this study have been presented by Adegbesan (1982).

No difficulties were encountered in fitting the models proposed in this study. Convergence was achieved quite rapidly in the final step. The maximum likelihood estimates of the parameters in the models including the rate constants obtained at each temperature are presented in Tables 3 to 7.

It should be noted that the kinetic parameters reported in Tables 4 to 7 include the Henry's law parameters as lumped by Eqs. 13 and 14. However, it is interesting to know that model C-1 provides estimates of the Henry's law parameters. These parameters can thus be applied to estimate the actual Arrhenius frequency factors and the activation energies of the reaction

Table 4. Rate Data for Model C-2

REACTION SCHEME	$A_1 \xrightarrow{k_{15},\ E_{15}} A_5$ (Maltenes) (Asphaltenes-coke)
REACTION MODEL	$\frac{dX_{A_1}}{dt} = -[k\acute{o}_{15}X_{A_1}\exp(-E'_{15}/RT)]\,p_{ox}^{m7}$ $\frac{dX_{A_5}}{dt} = -\frac{dX_{A_1}}{dt}$ $k\acute{o}_{\ell i} = Ho^{-mi}ko_{\ell j};\ E'_{\ell j} = E_{\ell j} - mi\ L$
Frequency Factor (h^{-1} . kPa^{-mi})	$k\acute{o}_{15}$ [h^{-1} . $kPa^{-0.41}$] 1.000 E + 08
Activation Energy (J/mol)	E'_{15} 81.927
Rate Constant (h^{-1} . kPa^{-mi})	k'_{15} [h^{-1} . $kPa^{-0.41}$]
423 K	8.360 E - 03
408 K	3.630 E - 03
393 K	1.490 E - 03
378 K	4.840 E - 03
333 K	3.030 E - 05
Order of Reaction with respect to Oxygen Partial Pressure . (mi)	m7 = 0.41

Table 5. Rate Data for Model C-3

REACTION SCHEME	$A_2 \xrightarrow{k_{26},\ E_{26}} A_6 \xrightarrow{k_{65},\ E_{65}} A_5$ (Oils) (Resins) (Asphaltenes-Coke)	
REACTION MODEL	$\frac{dX}{dt}{}_{A_2} = -[k\acute{o}_{26}X_{A_2}\ \exp(-E'_{26}/RT)]\ P_{ox}^{m5}$ $\frac{dX}{dt}{}_{A_6} = k\acute{o}_{26}X_{A_2}P_{ox}^{m5}\exp(-E'_{26}/RT) - k\acute{o}_{65}P_{ox}^{m6}X_{A_6}\exp(-E'_{65}/RT)$ $\frac{dX}{dt}{}_{A_5} = [k\acute{o}_{65}X_{A_6}\ \exp(-E'_{65}/RT)]\ P_{ox}^{m6}$ $k\acute{o}_{\ell j} = Ho^{-mi}ko_{\ell j};\ E'_{\ell j} = E_{\ell j} - mi\ L$	
Frequency Factor (h^{-1} . kPa^{-mi})	$k\acute{o}_{26}$ [$h^{-1}kPa^{-0.41}$] 2.638 E + 07	$k\acute{o}_{65}$ [$h^{-1}.kPa^{-0.50}$] 7.688 E + 08
Activation Energy (J/mol)	E'_{26} 77.234	E'_{65} 86.730
Rate Constant (h^{-1} . kPa^{-mi})	k'_{26} [$h^{-1}kPa^{-0.41}$]	k'_{65} [$h^{-1}kPa^{-0.50}$]
423 K	6.960 E-03	1.450 E-02
408 K	3.240 E-03	6.330 E-03
393 K	1.550 E-03	2.370 E-03
378 K	5.790 E-04	7.080 E-04
333 K	9.940 E-05	6.460 E-05
Order of Reaction with Respect to Oxygen Partial Pressure. (mi)	m5 = 0.41	m6 = 0.50

Table 6. Rate Data for Model C-4A

REACTION SCHEME	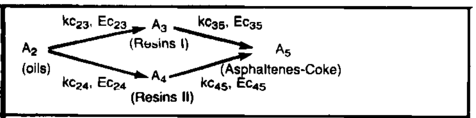			
REACTION MODEL	$\frac{dX_{A_2}}{dt} = -[k'co_{23}X_{A_2}\exp(-Ec'_{23}/RT) + k'co_{24}X_{A_2}\exp(-Ec'_{24}/RT)]\,p_{ox}^{m2}$ $\frac{dX_{A_3}}{dt} = [k'co_{23}X_{A_2}p_{ox}^{m2}\exp(-Ec'_{23}/RT) - k'co_{35}X_{A_3}p_{ox}^{m3}\exp(-Ec'_{35}/RT)]$ $\frac{dX_{A_4}}{dt} = [k'co_{24}X_{A_2}p_{ox}^{m2}\exp(-Ec'_{24}/RT) - k'co_{45}X_{A_3}p_{ox}^{m4}\exp(-Ec'_{45}/RT)]$ $\frac{dX_{A_5}}{dt} = [k'co_{35}X_{A_3}p_{ox}^{m3}\exp(-Ec'_{35}/RT) - k'co_{45}X_{A_3}p_{ox}^{m4}\exp(-Ec'_{45}/RT)]$ $k'co_{\ell j} = Ho^{-mi}\,kco_{\ell j};\ Ec'_{\ell j} = Ec'_{\ell j} - mi\ \ L$			
Frequency Factor (h^{-1} . kPa^{-mi})	$k'oc_{23}$ (h^{-1} . kPa^{-mi}) 1.813 E + 07	$k'oc_{24}$ (h^{-1} . $kPa^{-0.41}$) 4.637 E + 03	$k'oc_{35}$ (h^{-1} . $kPa^{-0.50}$) 1.939 E + 09	$k'oc_{45}$ (h^{-1} . $kPa^{-0.50}$) 4.483 E + 07
Activation Energy (J/mol)	Ec'_{23} 77.749	Ec'_{24} 52.377	Ec'_{35} 89.041	Ec'_{45} 79.135
Rate Constant (h^{-1} . kPa^{-mi})	kc'_{23} (h^{-1} . $kPa^{-0.41}$)	kc'_{24} (h^{-1} . $kPa^{-0.41}$)	kc'_{35} (h^{-1} . $kPa^{-0.50}$)	kc'_{45} (h^{-1} . $kPa^{-0.50}$)
423 K	4.429 E - 03	6.307 E - 03	2.370 E - 02	2.693 E - 02
408 K	1.500 E - 03	1.728 E - 03	7.966 E - 03	4.230 E - 03
393 K	5.390 E - 04	9.960 E - 04	2.777 E - 03	1.737 E - 03
378 K	4.868 E - 05	3.485 E - 04	7.865 E - 04	7.417 E - 04
333 K	9.695 E - 08	4.732 E - 05	7.064 E - 05	2.059 E - 05
Order of Reaction with respect to Oxygen Partial Pressure . (mi)	m2 = 0.41	m3 = 0.50	m4 = 0.50	

Table 7. Rate Data for Model C-4B

REACTION SCHEME	$A_2 \xrightarrow{k_{23},\ E_{23}} A_3 \xrightarrow{k_{34},\ E_{34}} A_4 \xrightarrow{k_{45},\ E_{45}} A_5$ (oils) (Resins I) (Resins II) (Asphaltenes-Coke)		
REACTION MODEL	$\frac{dX_{A_2}}{dt} = -[k'o_{23}X_{A_2}\exp(-E'_{23}/RT)]\,p_{ox}^{m2}$ $\frac{dX_{A_3}}{dt} = [k'o_{23}X_{A_2}p_{ox}^{m2}\exp(-E'_{23}/RT) - k'o_{23}X_{A_3}p_{ox}^{m3}\exp(-E'_{34}/RT)]$ $\frac{dX_{A_4}}{dt} = [k'o_{34}X_{A_3}p_{ox}^{m3}\exp(-E'_{34}/RT) - k'o_{45}X_{A_4}p_{ox}^{m4}\exp(-E'_{45}/RT)]$ $\frac{dX_{A_5}}{dt} = [k'o_{45}X_{A_4}\exp(-E'_{45}/RT)]\,p_{ox}^{m4}$ $k'o_{\ell j} = Ho^{-mi}\,ko_{\ell j};\ E'_{\ell j} = E_{\ell j} \cdot mi\ \ L$		
Frequency Factor (h^{-1} . kPa^{-mi})	$k'o_{23}$ (h^{-1} . $kPa^{-0.41}$) 1.164 E + 07	$k'o_{34}$ (h^{-1} . $kPa^{-0.50}$) 7.781 E + 07	$k'o_{45}$ (h^{-1} . $kPa^{-0.50}$) 3.918 E + 09
Activation Energy (J/mol)	E'_{23} 74.919	E'_{34} 4877.267	E'_{45} 89.141
Rate Constant (h^{-1} . kPa^{-mi})	k'_{23} [h^{-1} . $kPa^{-0.41}$]	k'_{34} [h^{-1} . $kPa^{-0.50}$)	k'_{45} (h^{-1} . $kPa^{-0.50}$)
423 K	7.060 E - 03	2.290 E - 02	3.810 E - 02
408 K	3.490 E - 03	1.060 E - 02	1.630 E - 02
393 K	1.500 E - 03	4.060 E - 03	5.990 E - 03
378 K	3.820 E - 04	1.170 E - 03	2.030 E - 03
333 K	1.540 E - 04	3.690 E - 04	2.180 E - 04
Order of Reaction with respect to Oxygen Partial Pressure . (mi)	m2 = 0.41	m3 = 0.50	m4 = 0.50

models and hence uncouple the effect of oxygen solubility on the kinetic parameters. It is the authors' belief that this is the first time in the technical literature that Henry's law parameters have been estimated in this manner.

Comparison of results with previous studies

It is important that the activation energies be positive and realistic. The following comments can be made on studies published in the literature regarding low-temperature oxidation of Athabasca bitumen:

- Very few studies have considered reaction schemes in which the major reaction components of the liquid phase were represented. In fact, reported studies have been qualitative in nature and no attempts were made to conduct systematic kinetic experiments.
- Kinetics parameters have not been reported for the overall rate of oxygen consumption.

However, data do exist in the literature for overall rate of oxygen consumption for low-temperature oxidation reactions of crude oils. For the overall rate, a comparison of literature data with those obtained in this study indicates that the activation energy, E (Table 3), of model C-1 for bitumen oxidation is much larger than those reported for crude oil oxidation in porous media (Adegbesan, 1982).

Overall, the activation energies reported for the proposed models (Tables 3–7) are positive and give reasonably accurate representations of the experimentally measured concentration vs. reaction time curves. These are discussed in detail in the following section.

Arrhenius plots and comparison of predicted and experimental data

Figure 8 shows the Arrhenius plot for model C-1 over the temperature range 333 to 423 K. A good correlation is observed

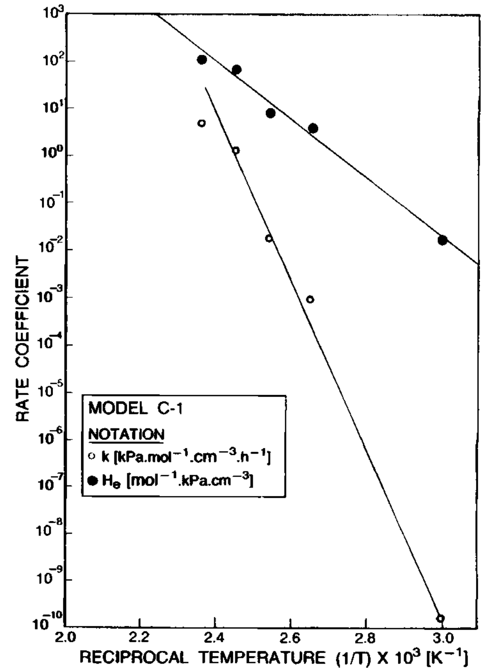

Figure 8. Model C-1: Reaction rate coefficient vs. inverse absolute temperature.

over the total temperature range. The plot of Henry's law coefficient vs. inverse absolute temperature is also given in Figure 8. This shows the expected linear relationships.

All the lumped-component models—C-2, C-3, C-4A, and C-4B—yield good predictions of the LTO reactions. More detailed results are presented in this section for model C-3 only as it is simpler than the four-component models and it yields excellent prediction of the LTO reactions. A detailed presentation for all the models is provided in a previous publication (Adegbesan, 1982). Figure 9 presents the Arrhenius plots for the reaction rate coefficients contained in model C-3. It is observed that the Arrhenius plots are linear at temperatures above 333 K. This implies that the model does not adequately represent the oxidation reactions at and below 333 K. This same behavior was noted for the two- and four-component models, and further experimental work is required to explain the change in reaction kinetics. The final parameter estimates presented in Tables 4–7 were determined using kinetic data obtained at temperatures above 333 K.

Figure 10 compares, at 408 K, the predicted concentration vs. reaction time curves of model C-3 with measured experimental data. This figure shows that the experimental concentration vs. reaction time curves were well reproduced by this model. Excellent reproductions of the concentration vs. time curves were also obtained at 423, 393, and 378 K. Similar prediction performances were also obtained for models C-2, C-4A, and C-4B in the temperature range 378 to 423 K. The fractional concentrations of the maltenes, the oils, the resins, and the asphaltenes-coke components were accurately predicted by the models.

Test for lack of fit

A fitted model is termed adequate to represent the data when the lack of fit variance is not significantly different from the error variance. The analysis of variance is shown in Table 8.

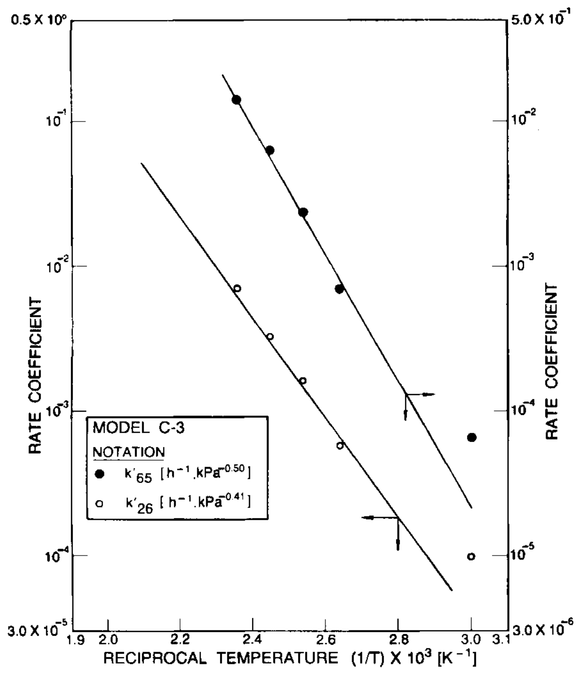

Figure 9. Model C-3: Reaction rate vs. inverse absolute temperature.

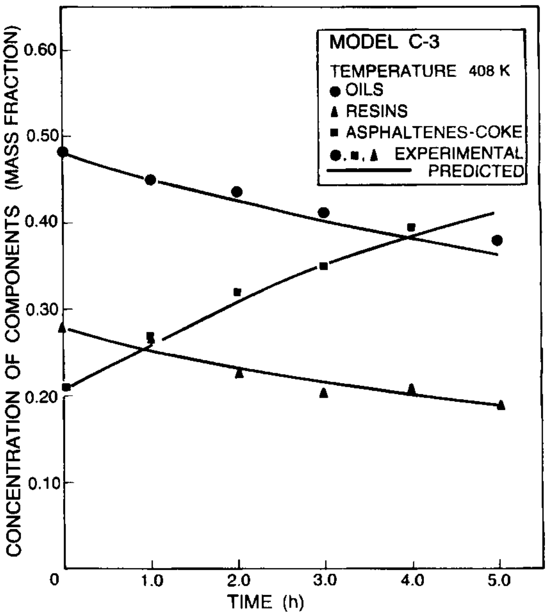

Figure 10. Predicted conversions of bitumen at 408 K by model C-3.

This table shows that the F ratios follow the F distribution with degrees of freedom at the 5% significance level. Thus, all the models proposed in this study are adequate.

Conclusions

The conclusions reached in this study may be summarized as follows:

1. Excellent agreement exists between the proposed models and the experimental data. This marks the first time in the technical literature that kinetic models have been established for the liquid phase reaction components involved in LTO reactions of oil sands bitumen.

2. A second-order dependency on oxygen partial pressure was estimated for the overall rate of consumption of oxygen. However, the SARA lumped-components reaction orders with respect to oxygen partial pressure were between 0 and 1.

3. A single reaction mechanism was found adequate for describing the overall rate of consumption of oxygen in the temperature range 333 to 423 K. However, for the reactions of the liquid phase lumped components, more than one mechanism may be assumed to take place. The mechanism describing the reactions in the temperature range 378 to 423 K does not adequately represent reactions occurring at the lower temperatures (at about 333 K).

4. Parameters were determined from experimental kinetic data for estimation of the solubility of oxygen in heavy oils or mixtures of complex hydrocarbons. In this study, an exponential expression was successfully used to estimate the solubility of oxygen in bitumen from collected kinetics data.

5. The use of statistical techniques in establishing reaction models was found to be very effective. The presence of linear dependencies among the measured response was detected using the eigenvalue-eigenvector method. The linear dependencies were removed by transformation of the multiresponse data using nonzero eigenvectors.

Table 8. Analysis for Lack of Fit

	Model				
	C-1	C-2	C-3	C-4A	C-4B
Residual					
Sum of squares	0.2246E-03	0.2317E-03	0.2794E-01	0.6231E-01	0.5502E-01
Degrees of freedom	49	44	42	38	40
Experimental Error					
Sum of squares	0.468E-05	0.2837E-03	0.4071E-03	0.9852E-03	0.9852E-03
Degrees of freedom (V_2)	3	3	3	3	3
Mean square (MSPE)	0.1560E-05	0.9455E-04	0.1357E-03	0.3284E-03	0.3284E-03
Lack of fit					
Sum of squares	0.2199E-03	0.2289E-01	0.2753E-01	0.6133E-01	0.5404E-01
Degrees of freedom (V_1)	46	41	39	35	37
Mean square (MSLF)	0.4781E-05	0.5583E-03	0.7059E-03	0.1752E-02	0.1460E-02
F-Test					
Variance ratio (MSLF/MSPE)	3.06	5.91	5.20	5.34	4.45
$F(V_2, V_2, 0.05)$	8.60	8.60	8.60	8.60	8.60
Model adequate?	Yes	Yes	Yes	Yes	Yes

Acknowledgment

The authors wish to thank Alberta Oil Sands Technology and Research Authority for financial support during this investigation. The authors also wish to thank Texaco Canada Resources Limited and Esso Resources Canada Limited for support during the preparation of this manuscript.

Notation

A = components of bitumen
A_1 = maltenes
A_2 = oils
A_3 = resins I
A_4 = resins II
A_5 = asphaltenes–coke
A_6 = resins = (resins I + resins II)
C = concentration of absorbing gas in liquid phase, kmol/m^3
C^* = interface value of C, kmol/m^3
C_H = total concentration of hydrocarbons, kmol/m^3
C_{O_2}, Cox = oxygen concentration in the liquid phase, kmol/m^3
C_j = concentration of component J in the liquid phase at time t = 0, kmol/m^3
E, Ec = Arrhenius activation energy, J/kmol
E', Ec' = lumped activation energy, J/kmol
G = molar flow rate, kmol/s
h^g = enthalpy per mole of gaseous component, Eq. 6, J
H = partial molar enthalpy of solution, Eq. 6, J
He = $He = p/C$, Henry's law coefficient, Pa · m^3/kmol
Ho = Henry's law preexponential factor, Pa · m^3/kmol
kc = kinetic rate constant, Pa^{-mi} · s^{-1}
ko, kco = Arrhenius frequency factor (preexponential factor), m^3/s · kmol
ko', $kc'o$ = lumped Arrhenius preexponential factor, Pa^{-mi} · s
K_L = liquid phase mass transfer coefficient, m/s
K_G = overall gas phase mass transfer coefficient, kmol · s/m · kg
L = heat absorbed in evaporation of 1 mol of gas from constant-temperature solution, J
m, mi = order of reaction with respect to oxygen
P = total pressure, Pa
p = partial pressure, Pa
P_{ox} = oxygen partial pressure, Pa
r = chemical reaction rate, kmol/m^3 · s
R = universal gas constant, Pa · m^3/kmol · K
t = time, s
T = temperature, K
V = partial molar volume of solution, Eq. 5, m^3
V_G = volume of gas phase in reactor, m^3
V_L = volume of liquid phase in reactor, m^3
X = mass fraction of component of bitumen: i = 1, maltenes; i = 2, oils; i = 3, resins I; i = 4, resins II; i = 5, asphaltenes–coke; i = 6, resins (=resins I + II)
Y = mole fraction of oxygen in gas phase or in reactor exit gas
Y_j = mole fraction of component j in gas phase or in reactor exit gas
Y_j^* = equilibrium mole fraction of component j in liquid phase
Y_{oj} = mole fraction of component j in reactor inlet gas
Y_{O_2}, in = mole fraction of oxygen in reactor inlet gas
Y_{O_2}, out = mole fraction of oxygen in reactor exit gas
z = compressibility factor of gas

Literature cited

Adegbesan, K. O., "Kinetic Study of Low-Temperature Oxidation of Athabasca Bitumen," Ph.D. Thesis, Univ. of Calgary, Alberta (1982).

Alexander, J. D., W. W. Martin, and J. N. Dews, "Factors Affecting Fuel Availability and Composition during *In Situ* Combustion," *J. Pet. Tech.*, p. 1154 (Oct., 1962).

Bennion, D. W., J. K. Donnelly, and R. G. Moore, "A Laboratory Investigation of Wet Combustion in the Athabasca Oil Sands," *The Oil Sands of Canada-Venezuela, 1977,* D. A. Redford and A. G. Winestock, eds. Canadian Inst. Mining and Metallurgy, Special Vol. **17,** 554 (1977).

Box, G. E. P., and N. R. Draper, "The Bayesian Estimation of Common Parameters from Several Responses," *Biometrika,* **52** (3 & 4) 335 (1966).

Box, G. E. P., W. G. Hunter, J. F. MacGregor, and J. Erjavec, "Some Problems Associated with the Analysis of Multiresponse Data," *Technometrics,* **15** (1) (Feb., 1973).

Bulmer, J. T., and J. Starr, "Syncrude Analytical Methods for Oil Sand and Bitumen Processing," Alberta Oil Sands Technology and Research Authority, Edmonton, Alberta (1979).

Burger, J. G., and B. C. Sahuquet, "Laboratory Research on Wet Combustion," *J. Pet. Tech.*, p. 1137 (1973).

Cram, P. J., and D. A. Redford, "Low-Temperature Oxidation Process For the Recovery of Bitumen," *The Oil Sands of Canada-Venezuela, 1977,* D. A. Redford and A. G. Winestock, eds., Canadian Inst. Mining and Metallurgy, Special Vol. **17,** 679 (1977).

Dabbous, M. K., and P. F. Fulton, "Low-Temperature Oxidation Reaction Kinetics and Effect on the *In Situ* Combustion Process," *Soc. Pet. Eng. J.*, p. 253 (June, 1974).

Denbigh, K. *The Principles of Chemical Equilibrium,* 3rd ed., Cambridge Univ. Press, p. 255 (1971).

Dietz, D. N. "Wet Underground Combustion, State of the Art," *J. Pet. Tech.*, p. 605, (May, 1970).

Dietz, D. N., and J. Weidjema, "Wet and Partially Quenched Combustion," *J. Pet. Tech.*, p. 411 (Apr., 1968).

Fassihi, R. M., W. E. Brigham, and H. J. Ramey, "The Reaction Kinetics of *In Situ* Combustion," Paper No. 9454 *55th Ann. Fall Tech. Conf. SPE at AIME*, Dallas, TX (Sept., 1980).

Morse, R. A., "Oil Recovery by Underground Combustion," U.S. Patent 2,793,696 (May, 1957).

Morton, F., and R. T. T. Bell, "The Low-Temperature Liquid Phase Oxidation of Hydrocarbon: A Literature Survey," *J. Inst. Petr.*, **44** (417) (Sept., 1958).

Moschopedis, S. E., and J. G. Speight, "Oxidation of a Bitumen," *Fuel*, **54**, 210 (July, 1975).

———, "An Investigation of Asphalt Preparation from Athabasca Bitumen," *Proc. Assn. Asphalt Paving Technologists*, **45**, 78 (1976a).

———, "Investigation of Hydrogen Bonding by Oxygen Functions in Athabasca Bitumen," *Fuel*, **55**, 187 (July, 1976b).

———, "The Effect of Air Blowing on the Properties and Constitution of a Natural Bitumen," *J. Materials Sci.*, **12**, 990 (1977).

Nelson, T. W., and J. S. McNiels, Jr., "Oil Recovery by *In Situ* Combustion," *Pet. Eng.*, **PB29** (July, 1956).

Reed, L., D. W. Reed, and J. Tracht, "Experimental Aspects of Reverse Combustion in Tar Sands," *AIME Petr. Trans.*, **219** (1960).

Showalter, W. E. "Combustion-Drive Tests," *AIME Petr. Trans.*, **228** (1963).

Smith, P. W., and Perkins, "Experimental and Numerical Simulation Studies of the Wet Combustion Recovery Process," *J. Can. Pet. Tech.*, **44**, (July–Sept., 1973).

Vorndran, L. D. L., A. J. Serres, J. K. Donnelly, R. G. Moore, and D. W. Bennion, "Bitumen Separation for Experimental Use," *Can. J. Chem. Eng.*, **58**, 580 (1980).

Walter, H., "Application of Heat for Recovery of Oil: Field Test Results and Possibility of Profitable Operation," *J. Pet. Tech.*, **16**, (Feb., 1977).

Manuscript received July 24, 1984, and revision received Feb. 3, 1986.